



## Dye Congo Red adsorptive decolorization by adsorbents obtained from *Trametes pubescens* pellets

Jing Si, Baokai Cui\*

*Institute of Microbiology, Beijing Forestry University, P.O. Box 61, Qinghuadong Road 35, Haidian District, Beijing 100083, P.R. China*

*Tel./Fax: +86 10 62336309; email: baokaicui@yahoo.com.cn*

Received 5 June 2012; Accepted 12 February 2013

---

### ABSTRACT

A design of various dyes decolorization was conducted with the adsorbents obtained from *Trametes pubescens* pellets in submerged cultures. The results demonstrated that the adsorbents prepared by moist heat sterilization exhibited preferable decolorization capacity on azo dye Congo Red. A maximum decolorization rate of Congo Red of 72.31% was observed, which was all around 2.25 times higher than that of anthraquinone dye Disperse Blue B at the same level. Moreover, the decolorization rate-dependent influencing factors, i.e. salinity, Tween80, temperature, pH, and dye concentration, were optimized by Box–Behnken full factorial design. When they were 1.06% (*m/V*), 3.50% (*V/V*), 41.0°C, 6.15, and 114.34 mg/L respectively, the decolorization rate was up to 100% after a 7-day incubation period. Adsorptive decolorization was caused by the electrostatic forces between dye molecules and adsorbents obtained from *T. pubescens* pellets, amido group played a major role during the biosorption process, and this course did not alter any functional groups at all, as evidenced by fourier transform infrared spectroscopy, chemical modifications, and scanning electron microscope data. All the results indicated that the adsorbents performed well at lowering the possible limitations arising out of the poor stability and enhancing convenient operability.

*Keywords:* *Trametes pubescens* pellet adsorbent; Dye adsorptive decolorization; Moist heat sterilization; Box–Behnken full factorial design; Biosorption characterization

---

### 1. Introduction

Nowadays, dyes have been used increasingly in the textile and dyeing industries because of their ease and cost-effectiveness in synthesis, firmness, high stability to light, temperature, detergent, microbial attack, and variety in color [1]. Over  $7 \times 10^5$  ton and approximately 10,000 different dyes and pigments are produced annually worldwide, about 10% of which may be found in wastewater [2]. Color being the most

discernable indicator of pollution in aqueous environment, is the first to attract the attention of even an environmentally indifferent person [3]. It interferes with penetration of sunlight into water, retards photosynthesis, inhibits the growth of aquatic biota and disrupts gas solubility in water bodies [4,5]. In addition, many dyes are believed to be toxic or to be prepared from known carcinogens such as benzidine or other aromatic compounds that might be formed as a result of microbial metabolism [6,7]. Hence, removal of these dyes from effluents is of major scientific interest.

\*Corresponding author.

Many conventional methods are available for wastewater removal including adsorption on activated carbon, electrokinetic coagulation, filtration, chemical flocculation, chemical oxidation (ozonation, hydrogen peroxide, and chlorine), deep-well injection, ion exchange, incineration, solvent extraction, Fenton agents, irradiation, and so on [8,9]. However, high cost and secondary pollution of these physicochemical treatments have stimulated increasing interest to use biological methods for wastewater treatment, which are much cheaper and environment-friendly [10,11]. A large number of bacteria, plants, and fungi are well known to degrade textiles wastewater. They are able to depolymerize and even mineralize the dyes, and have the peculiar capability to synthesize a series of relevant hydrolytic and oxidative extracellular enzymes [12–14]. However, the extracellular enzymes sometimes displayed instability and deactivation, and one solution to this problem is biosorption treatment based on dead micro-organisms or plants [15]. Biosorption is an attractive method for the treatment of wastewater as its low cost, simplicity of design, ease of operation, and insensitivity to toxic pollutants [16]. This process is attributed to the adsorbent's relatively heterogeneous surface area and high binding affinity of ionic exchanging sites. Extracellular polymers on the cell wall consist of surface functional groups, such as carboxyl, phosphate, and amino, which are considered to be responsible for removing anionic species such as dye and other contaminants via electrostatic interaction or hydrogen bonding [17]. Sulaymon et al. found that the binding capacity and desorbing efficiency of dead micro-organisms separated from sludge were significantly higher than that of live micro-organisms at the same tested conditions [18].

In the last decade, there has been an increasing interest to find cheaper and more easily obtained adsorbents. Previous studies concerning biosorption of dye removal were mostly centered on certain bacteria and plants such as rice husk, *Posidonia oceanic* and *Pseudomonas* [16–19]. However, there were scanty studies on the dye adsorption by fungi, and mainly focused on *Aspergillus* and *Penicillium* [20,21]. Only a few studies of dead macro-fungi applied to dye adsorption were carried out [22]. To date, several researches were conducted to decolorize dyes by macro-fungus *Trametes pubescens* assisted with immobilization treatment, physicochemical methods or its degraded enzymes [23–25]. However, no studies on the biosorption of azo dyes by dead macro-fungus *T. pubescens* were reported.

Therefore, this paper reports the dye uptake potentials of dead fungal pellets from *T. pubescens* prepared by moist heat sterilization treatment. The decolorization

rate-dependent influencing factors, viz. salinity, Tween80, temperature, pH, and dye concentration, were optimized to enhance the dye decolorization via Box–Behnken full factorial design (BBD). Additionally, biosorption mechanism, modification of functional groups, and morphology changes of cell walls were also characterized by Fourier transform infrared spectroscopy (FTIR) and scanning electron microscope (SEM).

## 2. Materials and methods

### 2.1. Dyes

Table 1 presents the dyes used in this study and their color index numbers, chemical classes, and wavelengths at pH 7.0; the dye solutions were prepared by filtration through a 0.22  $\mu\text{m}$  membrane to remove bacteria before use.

### 2.2. Fungus and inocula preparation

*T. pubescens* is a common white rot fungus and it has a wide distribution in China [26,27]. Its strain Cui 7571 used in the present study was collected from Guangdong Province of China and maintained through periodic (monthly) transfer on yeast extract glucose agar (YGA) at 4°C. The YGA medium used for the experiment contained (g/L of distilled water): yeast extract 5, glucose 20, agar 20,  $\text{KH}_2\text{PO}_4$  1,  $\text{MgSO}_4 \cdot 7\text{H}_2\text{O}$  0.5,  $\text{ZnSO}_4 \cdot 7\text{H}_2\text{O}$  0.05 and Vitamin B1 0.01, and the pH value of the medium was adjusted to 5.0 before sterilization.

Prior to use, the stored fungal strain was inoculated onto the newly prepared YGA plates and grown at 28°C statically. Five mycelial disks (1 cm diameter) were removed from the peripheral region of the YGA plates and then used to inoculate into a 250-mL Erlenmeyer flask containing 100 mL of yeast extract glucose medium (YG, identical to YGA without agar). The cultures were incubated at 28°C and 150 rpm for five days, and then they were homogenized using an Ace Homogenizer (Hengao Co., Tianjin, China) at 5,000 rpm for 30 s. The homogenized suspensions were prepared as inocula for next study.

### 2.3. Adsorbents preparation and FTIR analysis

An aliquot of 10 mL of inocula (0.087 g, dry weight) was inoculated into a 250 mL Erlenmeyer flask containing 100 mL of YG medium, and incubated at 28°C and 150 rpm. The cultures were harvested after five days and killed by moist heat sterilization at 121°C for 20 min. After the supernatant was removed by centrifugation at 12,000 rpm for 20 min, the pellets

Table 1  
Decolorization of chemically various dyes by the adsorbents obtained from *Trametes pubescens* pellets

Dye	Color index number	Chemical class	Wavelength (pH7.0)	Decolorization rate (%)	
				Adsorbents	Pellets
Reactive Brilliant Blue X-BR	61,205	Anthraquinone	603	34.50	44.13
Disperse Blue B	61,500	Anthraquinone	640	32.15	46.15
Congo Red	22,120	Azo	497	72.31	73.34
Methyl Red	13,020	Azo	523	66.25	62.23
Sudan Black B	26,150	Azo	498	62.51	68.32
Trypan Blue	23,850	Azo	607	63.64	67.28
Neutral Red	50,040	Heterocycle	553	47.94	69.84
Methylene Blue	52,015	Thiazine	661	45.54	14.21
Crystal Violet	42,555	Triphenylmethane	595	58.33	65.20
Ethyl Violet	42,600	Triphenylmethane	596	57.48	59.92
Victoria Blue	44,045	Triphenylmethane	599	50.51	53.45
Brilliant Green	42,040	Triphenylmethane	623	51.28	57.12

were rinsed four times, dried at 105°C to constant weight, triturated, and sieved with 100 mesh screen. Then the dry powders were the adsorbents used for further analysis.

To determine the functional groups distribution the FTIR analysis was done on Perkin-Elmer, spectrum one instrument in the mid IR region of 400–4,000 cm<sup>-1</sup> with 16 scan speed (Spectrum One, Perkin Elmer, USA). Discs were prepared by first mixing 2 mg dried samples with 200 mg KBr in an agate mortar. The resulting mixture was pressed at 10 MPa for 3 min using a YP-2 tablet press (Shanghai, China).

#### 2.4. Dye decolorization

An aliquot of 50 mg of dry powders was inoculated into a 250 mL Erlenmeyer flask containing 100 mL of 100 mg/L of selected dyes solutions, and the cultures were incubated for 7 days at 28°C and 150 rpm in the dark to avoid dye polymerization by light. Uninoculated (without dry powders) flasks and inoculated (with fresh pellets) flasks with addition of media YGA were selected as controls under identical conditions. Experiments were all performed in triplicate.

Ten milliliters of samples were withdrawn and centrifuged at 12,000 rpm for 15 min, and then the supernatant was used for decolorization capacity determination. The UV-Visible adsorption spectra of the dyes solutions before and after decolorization by the adsorbents obtained from *T. pubescens* pellets were recorded between 200 and 800 nm with a UV-Visible spectrophotometer (UNICO 4802, Younike Co., Shanghai, China). Then the decolorization rate (%) was expressed in terms of percentage and calculated as follows:

$$\text{Decolorization rate (\%)} = \frac{[(\text{initial absorbance} - \text{final absorbance}) / \text{initial absorbance}] \times 100}{100}$$

#### 2.5. Decolorization rate-dependent influencing factors optimization

One BBD was carried out in order to optimize the factors, i.e. salinity (NaCl, m/V, %), Tween80 (V/V, %), temperature (°C), pH, and dye concentration (mg/L), which influenced the target dye decolorization capacity by the adsorbents obtained from *T. pubescens* pellets. Amounts of these factors and experimental design of BBD were specified according to Table 2 for each treatment. After sterilization, a 100 mL volume of the target dye solution, with salinity, Tween80, pH, and dye concentration as specified, was pipette into a 250 mL Erlenmeyer flask. The cultures were inoculated with 50 mg of dry powders and incubated at 150 rpm in dark and specified temperature for 7 days. Experiments were all performed in triplicate. Decolorization rate (%) determination and expression were mentioned in Section 2.4.

The main effects for each of the factors evaluated on the response were:

$$\beta_i = (y_i^+) - (y_i^-) \quad (1)$$

where  $\beta_i$  was the effect of the *i*th factor on the response,  $y_i^+$  and  $y_i^-$  were the mean responses for the upper (+) and the lower (-) levels of the *i*th factor, respectively. Interactions of two factors were also

calculated by this equation. The general equation was a first-degree polynomial:

$$Y = \beta_0 + \sum \beta_i X_i + \sum \beta_{ij} X_{ij} + \varepsilon \quad (2)$$

where  $Y$  was the estimated response,  $\beta_0$  was the general mean,  $\sum \beta_i X_i$  was the sum of main effects of the factors,  $\sum \beta_{ij} X_{ij}$  was the sum of two-factor interaction effects, and  $\varepsilon$  was the lack of fit of the model (error).

### 2.6. Chemical modification

An aliquot of 1.0 g of adsorbents inoculated into the 250 mL Erlenmeyer flask containing 75 mL of acetone was heated to reflux for 6 h to scavenge fungal surface lipids. Another aliquot of 1.0 g of adsorbents inoculated into the 250 mL Erlenmeyer flask containing 40 mL of triethyl phosphate and 30 mL of nitromethane was heated to reflux for 6 h for phosphate esterification. Another aliquot of 1.0 g of adsorbents inoculated into the 250-mL Erlenmeyer flask containing 20 mL of methanal and 40 mL of methanoic acid was incubated at 28°C and 150 rpm for 6 h for amido methylation. Another aliquot of 1.0 g of adsorbents inoculated into the 250-mL Erlenmeyer flask containing 60 mL of acetic anhydride was heated to reflux for 10 h for amido acetylation. Another aliquot of 2.0 g of adsorbents inoculated into the 250-mL Erlenmeyer flask containing 130 mL of methanol and 1.2 mL of concentrated hydrochloric acid was incubated at 28°C and 150 rpm for 6 h for carboxyl esterification.

The modified adsorbents by chemical methods were recorded as (a) lipid removal, (b) phosphate esterification, (c) amido methylation, (d) amido acetylation, and (e) carboxyl esterification, respectively. All of them were centrifuged at 12,000 rpm for 20 min, and the water-insoluble fractions were dried at 105°C to constant weight for dye decolorization. Target dye solution containing adsorbents without any chemical modifications was selected as control. Experiments were all performed in triplicate. Decolorization rate (%) determination and expression were mentioned in Section 2.4.

### 2.7. Biosorption characterization

Once complete decolorization was achieved, the adsorbents were taken photomicrographs by SEM to detect the structural modifications of cell walls. Samples of untreated and treated adsorbents were prepared by attaching these on a specimen stub using double-coated tape and sputter-coated with AuPd prior to imaging with a HITACHI-S3400N SEM

(Hitechi Ltd., Tokyo, Japan) using an accelerating voltage of 2 kV.

FTIR analysis of the adsorbents after complete dye decolorization followed the Section 2.3.

### 2.8. Statistical data analysis

The results obtained during experimentation were expressed in terms of means and standard error means. Data were subjected to statistical analysis of one-way analysis of variance (ANOVA),  $T$ -test and LSD test by using Microsoft excel and MSTAT softwares. Correlation between different parameters was calculated by SPSS software. Probability ( $p$  value) less than 0.05 or 0.01 was considered significant or highly significant, respectively. The results obtained from BBD were tested by Design Expert V.7.1.6. Software.

## 3. Results and discussion

### 3.1. FTIR analysis

To verify the functional groups distribution of dead fungal adsorbent surface, the FTIR analysis was conducted primarily. As shown in Fig. 1(a), the FTIR spectrum of adsorbent obtained from *T. pubescens* pellets displayed peaks at 3,284 and 1,509  $\text{cm}^{-1}$  indicating  $-\text{N}-\text{H}$  stretching. Peaks at 3,000–3,500, 1,617, and 1,232  $\text{cm}^{-1}$  displayed  $-\text{C}=\text{O}-$  stretching. The stretching vibrations at 1,145 and 1,022  $\text{cm}^{-1}$  represented  $-\text{P}=\text{O}$  and  $-\text{P}-\text{O}$  stretching, respectively. This spectrum was elucidated according to the previously described researches [28–31]. In order to explore the contribution of surface functional groups during the dye biosorption, the chemical modifications were implemented in Section 3.4.

### 3.2. Dye decolorization

To confirm the enhancement in adsorptive decolorization capacities of various dyes due to the different treatments, i.e. adsorbents obtained from *T. pubescens* pellets prepared by moist heat sterilization and fresh pellets of *T. pubescens*, the various dyes solutions were submitted to shaking cultivation at 28°C and 150 rpm for 7 days and the decolorization rates of which were displayed in Table 1.

When the 12 various dyes were subjected to the adsorbents treatment, the cultures turned light color from initial dark hue, which further became colorless. An apparent increase in azo dye Congo Red decolorization efficiency occurred, and a maximum decolorization rate of 72.31% was observed after a 7-day incubation period, which was all around

Table 2

Box–Behnken full factorial design to investigate the influences of five selected variables ( $X_1$ ,  $X_2$ ,  $X_3$ ,  $X_4$ , and  $X_5$ ) on azo dye Congo Red decolorization rate (%) by the adsorbents obtained from *Trametes pubescens* pellets

Indications	Factors		Low level	High level
$X_1$	Salinity (NaCl, m/V, %)		0.50	5.00
$X_2$	Tween80 (V/V, %)		1.00	3.50
$X_3$	Temperature (°C)		30.0	150.0
$X_4$	pH		1.0	10.0
$X_5$	Dye concentration (mg/L)		20.0	500.0

Run number	$X_1$	$X_2$	$X_3$	$X_4$	$X_5$	Dye decolorization rate (%)
1	2.75	1.00	90.0	10.0	260.0	80.37
2	5.00	2.25	90.0	5.5	500.0	80.69
3	5.00	2.25	90.0	5.5	20.0	83.74
4	2.75	2.25	90.0	1.0	20.0	80.68
5	0.50	2.25	90.0	1.0	260.0	77.38
6	0.50	3.50	90.0	5.5	260.0	94.23
7	5.00	2.25	30.0	5.5	260.0	87.32
8	2.75	2.25	150.0	10.0	260.0	75.97
9	2.75	2.25	30.0	5.5	500.0	77.60
10	2.75	3.50	30.0	5.5	260.0	95.64
11	2.75	1.00	90.0	5.5	20.0	89.47
12	2.75	3.50	90.0	5.5	20.0	93.57
13	2.75	2.25	30.0	1.0	260.0	79.12
14	2.75	2.25	90.0	5.5	260.0	93.32
15	0.50	2.25	90.0	5.5	500.0	77.45
16	2.75	2.25	90.0	5.5	260.0	94.38
17	5.00	1.00	90.0	5.5	260.0	89.47
18	2.75	2.25	90.0	10.0	20.0	78.53
19	0.50	2.25	30.0	5.5	260.0	89.21
20	0.50	1.00	90.0	5.5	260.0	85.36
21	2.75	2.25	90.0	5.5	260.0	95.15
22	2.75	3.50	150.0	5.5	260.0	84.21
23	2.75	2.25	30.0	10.0	260.0	78.20
24	2.75	1.00	90.0	1.0	260.0	77.57
25	2.75	2.25	90.0	5.5	260.0	94.63
26	2.75	2.25	90.0	1.0	500.0	68.35
27	0.50	2.25	90.0	5.5	20.0	94.57
28	2.75	2.25	30.0	5.5	20.0	90.52
29	2.75	2.25	150.0	1.0	260.0	75.51
30	2.75	1.00	90.0	5.5	500.0	78.24
31	0.50	2.25	90.0	10.0	260.0	82.56
32	5.00	2.25	90.0	10.0	260.0	74.27
33	2.75	2.25	90.0	5.5	260.0	94.97
34	2.75	2.25	90.0	5.5	260.0	94.84
35	2.75	2.25	90.0	10.0	500.0	70.25
36	2.75	3.50	90.0	10.0	260.0	80.12
37	0.50	2.25	150.0	5.5	260.0	86.39
38	5.00	2.25	150.0	5.5	260.0	84.54
39	2.75	2.25	150.0	5.5	20.0	85.36

(Continued)

Table 2 (continued)

Run number	X <sub>1</sub>	X <sub>2</sub>	X <sub>3</sub>	X <sub>4</sub>	X <sub>5</sub>	Dye decolorization rate (%)
40	5.00	2.25	90.0	1.0	260.0	80.37
41	2.75	1.00	150.0	5.5	260.0	90.24
42	5.00	3.50	90.0	5.5	260.0	86.91
43	2.75	3.50	90.0	5.5	500.0	81.65
44	2.75	3.50	90.0	1.0	260.0	83.64
45	2.75	1.00	30.0	5.5	260.0	83.52
46	2.75	2.25	150.0	5.5	500.0	78.35

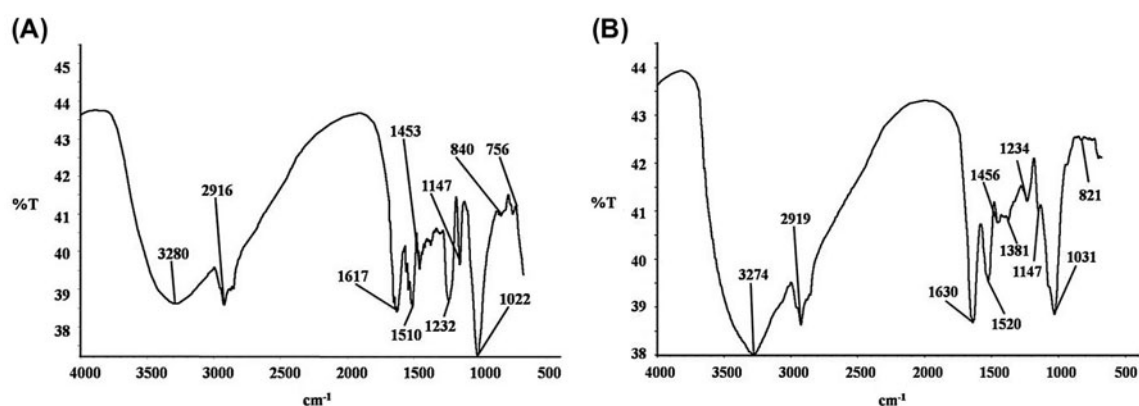


Fig. 1. FTIR spectra of the adsorbents obtained from *Trametes pubescens* pellets (A) before dye decolorization and (B) after dye decolorization.

2.25-fold higher than that of anthraquinone dye Disperse Blue B at the same level. Therefore, the azo dye Congo Red was selected as the target dye for the next experiment.

It is well known that industrial effluents generally contain a mixture of dyes and so, nonspecific method of decolorization is a requirement [22]. Because various chromophores were present in different dyes, other special factors could be responsible for the higher dye decolorization capacity. One factor was that the nonspecific property of the fungal strain caused an increase in cell permeability and mass transfer speed, thus leading to an increase in dye decolorization rate [32]. The other factor was that there existed one biosorption mechanism between dye molecules and adsorbents, which caused the dye decolorization course to occur [33,34]. Hence, these results suggested that the adsorbents obtained from *T. pubescens* pellets had potentials to decolorize textile dyes with different chemical structures, which could be developed into novel bioremediation strategies.

Furthermore, compared to the general treatment with fresh *T. pubescens* pellets, no dramatic variations were observed from the experimental decolorization

rates by the adsorbents obtained from *T. pubescens* pellets. Thus, the results also indicated that the treatment by adsorbents obtained from dead fungal pellets performed well at lowering the possible limitations arising out of the poor stability and enhancing convenient operability for dye decolorization.

### 3.3. Decolorization rate-dependent influencing factors optimization

Compared with the traditional “one-factor at a time” technique, statistically based experimental design is a more efficient approach to deal with a large number of variables [35,36]. As a useful statistical technique, BBD has been applied to optimization of medium components and conditions widely and successfully [37,38]. In this study, the five factors, viz. salinity (NaCl, *m/V*, %), Tween80 (*V/V*, %), temperature (°C), pH, and dye concentration (mg/L), were chosen on the basis of previous studies [37,39–41], and they were optimized to enhance the target dye Congo Red decolorization rate by the adsorbents obtained from *T. pubescens* pellets.

Table 3  
Statistical analysis of the results obtained from Box–Behnken full factorial design<sup>a</sup>

Source	Sum of squares	$d_f$	Mean square	F value	p Value
Model	2355.128000	20	117.756400	313.891000	0.0000**
$X_1$ —Salinity	24.601600	1	24.601600	65.577950	0.0000**
$X_2$ —Tween80	41.377060	1	41.377060	110.294600	0.0000**
$X_3$ —Temperature	26.419600	1	26.419600	70.424000	0.0000**
$X_4$ —pH	0.345156	1	0.345156	0.920047	0.3466
$X_5$ —Dye concentration	439.531200	1	439.531200	1171.613000	0.0000**
$X_1X_2$	32.661220	1	32.661220	87.061660	0.0000**
$X_1X_3$	0.000400	1	0.000400	0.001066	0.9742
$X_1X_4$	31.809600	1	31.809600	84.791570	0.0000**
$X_1X_5$	49.491230	1	49.491230	131.923700	0.0000**
$X_2X_3$	82.355630	1	82.355630	219.526900	0.0000**
$X_2X_4$	9.985600	1	9.985600	26.617580	0.0000**
$X_2X_5$	0.119025	1	0.119025	0.317273	0.5783
$X_3X_4$	0.476100	1	0.476100	1.269091	0.2706
$X_3X_5$	8.732025	1	8.732025	23.276060	0.0000**
$X_4X_5$	4.100625	1	4.100625	10.930610	0.0029**
$X_1^2$	99.974440	1	99.974440	266.491500	0.0000**
$X_2^2$	26.384740	1	26.384740	70.331080	0.0000**
$X_3^2$	172.660000	1	172.660000	460.242100	0.0000**
$X_4^2$	1403.653000	1	1403.653000	3741.573000	0.0000**
$X_5^2$	448.815900	1	448.815900	1196.362000	0.0000**
Residual	9.378762	25	0.375150	—	—
Lack of fit	7.210079	20	0.360504	0.831159	0.6566
Pure error	2.168683	5	0.433737	—	—
Corrected total	2364.506000	45	—	—	—
Std. Dev. = 0.612495			$R^2 = 0.996034$		
Mean = 84.313700			Adj. $R^2 = 0.992860$		
C.V. % = 0.726448			Pred. $R^2 = 0.986482$		
Press = 31.963220			Adeq. precision = 65.735800		

<sup>a</sup>\*\* $p < 0.01$ , highly significant; \* $p < 0.05$ , significant.

Table 2 listed the levels and actual values of the five variables as well as the experimental design and results of BBD. A total number of 46 runs were required for the optimum experimentation. Based on the levels of five variables and the experimental results, the statistical analysis was summarized in Table 3 by Design Expert V.7.1.6. Software analysis. The model terms of  $X_1$ ,  $X_2$ ,  $X_3$ ,  $X_5$ ,  $X_1X_2$ ,  $X_1X_4$ ,  $X_1X_5$ ,  $X_2X_3$ ,  $X_2X_4$ ,  $X_3X_5$ ,  $X_4X_5$ ,  $X_1^2$ ,  $X_2^2$ ,  $X_3^2$ ,  $X_4^2$ , and  $X_5^2$  were highly significant ( $p < 0.01$ ), but  $X_4$  and the interactive effects of  $X_1X_3$ ,  $X_2X_5$  and  $X_3X_4$  were not significant ( $p > 0.05$ ). It meant that salinity, Tween80, temperature, and dye concentration as well as their interactions had remarkable effects on Congo Red decolorization rate, and this model was applicable to the optimum experimentation. In addition, the multiple regression model obtained from dye decolorization gave the following second-order polynomial equation:

$$\begin{aligned}
 Y = & 94.55 - 1.24 \times X_1 + 1.61 \times X_2 - 1.28 \times X_3 \\
 & - 0.15 \times X_4 - 5.24 \times X_5 - 2.86 \times X_1X_2 + 0.01 \\
 & \times X_1X_3 - 2.82 \times X_1X_4 + 3.52 \times X_1X_5 - 4.54 \\
 & \times X_2X_3 - 1.58 \times X_2X_4 - 0.17 \times X_2X_5 + 0.34 \\
 & \times X_3X_4 + 1.48 \times X_3X_5 + 1.01 \times X_4X_5 - 3.38 \\
 & \times X_1^2 - 1.74 \times X_2^2 - 4.45 \times X_3^2 - 12.68 \times X_4^2 \\
 & - 7.17 \times X_5^2
 \end{aligned} \quad (3)$$

In the above-mentioned Eq. (3),  $Y$  was the target dye Congo Red decolorization rate (%) as well as  $X_1$ ,  $X_2$ ,  $X_3$ ,  $X_4$  and  $X_5$  were the coded levels of salinity (NaCl,  $m/V$ , %), Tween80 ( $V/V$ , %), temperature ( $^{\circ}C$ ), pH, and dye concentration (mg/L), respectively. The equation represented the mathematical model relating the dye decolorization rate with the independent

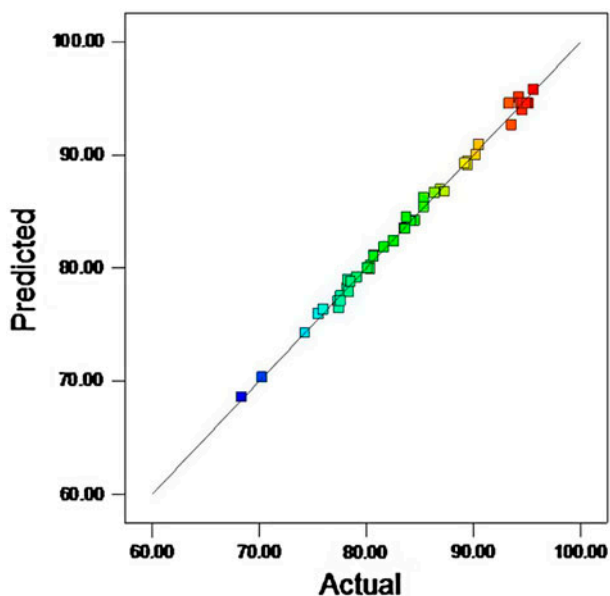


Fig. 2. The parity plot showing the distribution of experimental vs. predicted values of azo dye Congo Red decolorization rate.

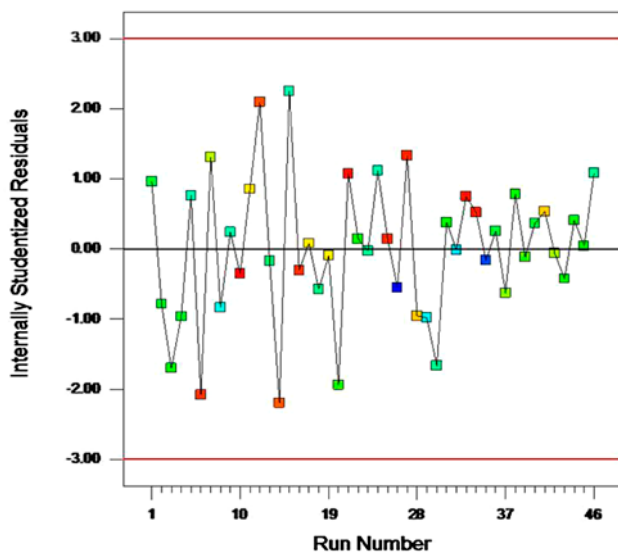


Fig. 3. Residual vs. the run number.

process variables  $X_1$  to  $X_5$ , and the second-order polynomial coefficient for each term of the equation was determined through multiple regression analysis using Design Expert V.7.1.6. Software. Since the regression equation obtained from ANOVA displayed that the multiple correlation coefficient  $R^2$  was 0.996034, it seemed to be that the model could explain 99.6034% variation in the response. The value of the adjusted determination coefficient ( $Adj. R^2 = 0.992860$ ) was also very high to advocate for a high significance

of model. The model  $F$  value of 313.891000 implied the model to be significant and was calculated as the ratio of mean square regression and mean square residual. According to the statistical results, the above model was adequate to predict the dye decolorization rate within the range of variables studied.

As presented in Fig. 2, the parity plot demonstrated that the distribution of the actual values, which was defined as the difference between the observed and the predicted, could form a straight line, and these residual values were normally distributed on both sides of the line. It revealed that experimental point was reasonably aligned with the predicted value.

Fig. 3 showed that the residuals distributed randomly about zero, suggesting that the regression terms were not correlated with one another. This plot ruled out the impact of run number which might influence the results.

The contour plots were generally the graphical representations of regression equation, and they were demonstrated in Fig. 4. The main goal of response surface was to track for the optimum values of the variables efficiently such that the response was maximized. Each contour curve plot represented an infinite number of combinations of two variables with the others maintained at their respective zero level. From the contour plots, it was easy and convenient to understand the interactions between two factors and also locate their optimum levels. The circular contour plots of response surfaces implied that the interaction was negligible between the corresponding variables. An elliptical or saddle nature of the contour plots indicated that the significance of the interactions between the corresponding variables. Contour plots in Fig. 4 displayed that there were significant mutual interactions between salinity and Tween80 ( $X_1X_2$ ) (Fig. 4(a)), salinity and pH ( $X_1X_4$ ) (Fig. 4(c)), salinity and dye concentration ( $X_1X_5$ ) (Fig. 4(d)), Tween80 and temperature ( $X_2X_3$ ) (Fig. 4(e)), Tween80 and pH ( $X_2X_4$ ) (Fig. 4(f)), temperature and dye concentration ( $X_3X_5$ ) (Fig. 4(i)) as well as pH and dye concentration ( $X_4X_5$ ) (Fig. 4(j)). However, no obvious interactions of salinity and temperature ( $X_1X_3$ ) (Fig. 4(b)), Tween80 and dye concentration ( $X_2X_5$ ) (Fig. 4(g)), as well as temperature and pH ( $X_3X_4$ ) (Fig. 4(h)) were observed from the relatively circular nature of contour plots.

The optimal conditions were extracted by Design Expert V.7.1.6. Software with its optimization menus: salinity 1.06% ( $m/V$ ), Tween80 3.50% ( $V/V$ ), temperature 41.0°C, pH 6.15, and dye concentration 114.34 mg/L, and then the azo dye Congo Red decolorization rate reached to its peak of 100% after 7 days of incubation. The validation experiment showed that

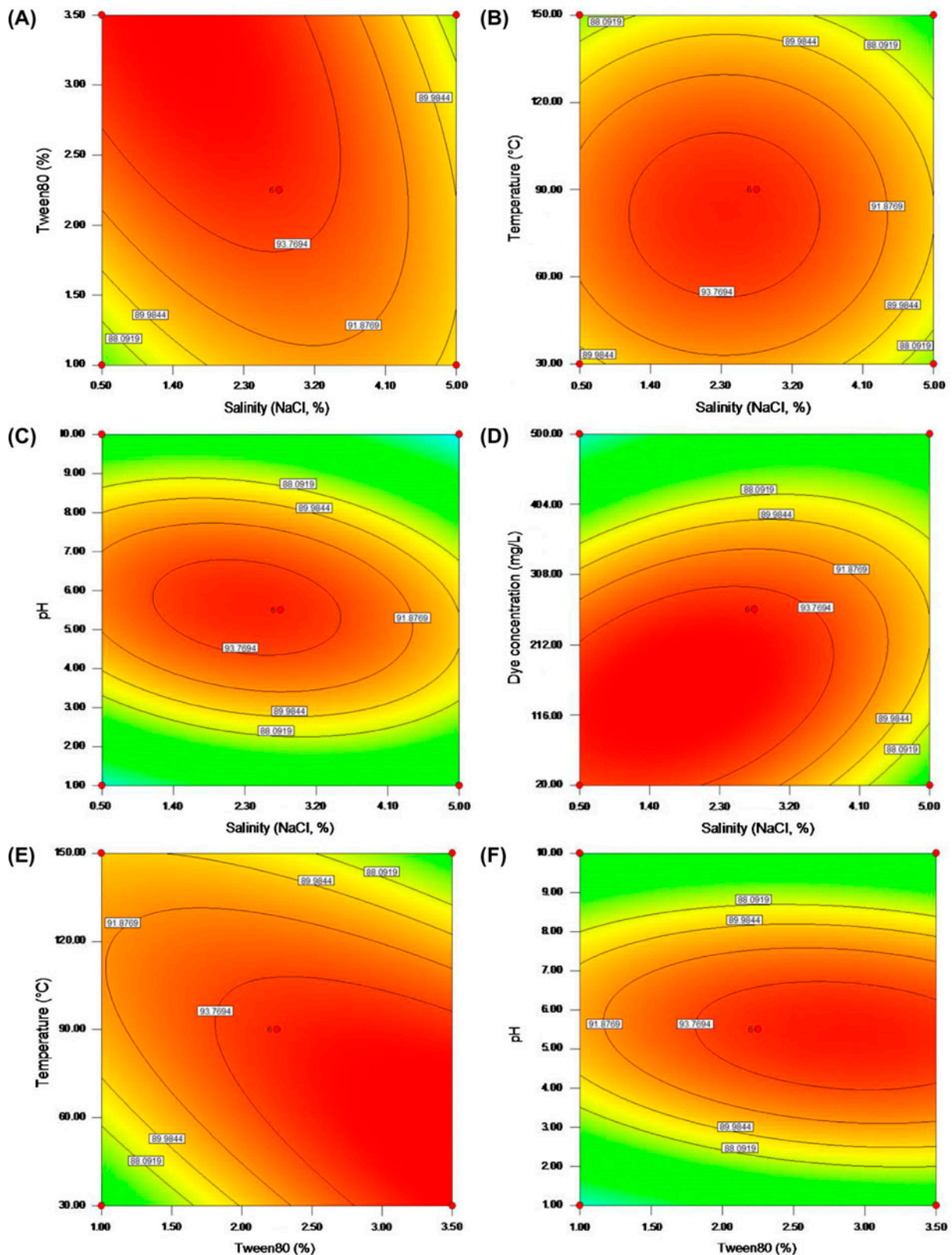


Fig. 4. The contour plots of Box–Behnken full factorial design (A) salinity ( $X_1$ ) and Tween80 ( $X_2$ ) (B) salinity ( $X_1$ ) and temperature ( $X_3$ ) (C) salinity ( $X_1$ ) and pH ( $X_4$ ) (D) salinity ( $X_1$ ) and dye concentration ( $X_5$ ) (E) Tween80 ( $X_2$ ) and temperature ( $X_3$ ) (F) Tween80 ( $X_2$ ) and pH ( $X_4$ ) (G) Tween80 ( $X_2$ ) and dye concentration ( $X_5$ ) (H) temperature ( $X_3$ ) and pH ( $X_4$ ) (I) temperature ( $X_3$ ) and dye concentration ( $X_5$ ), as well as (J) pH ( $X_4$ ) and dye concentration ( $X_5$ ). Other variables were held at zero level.

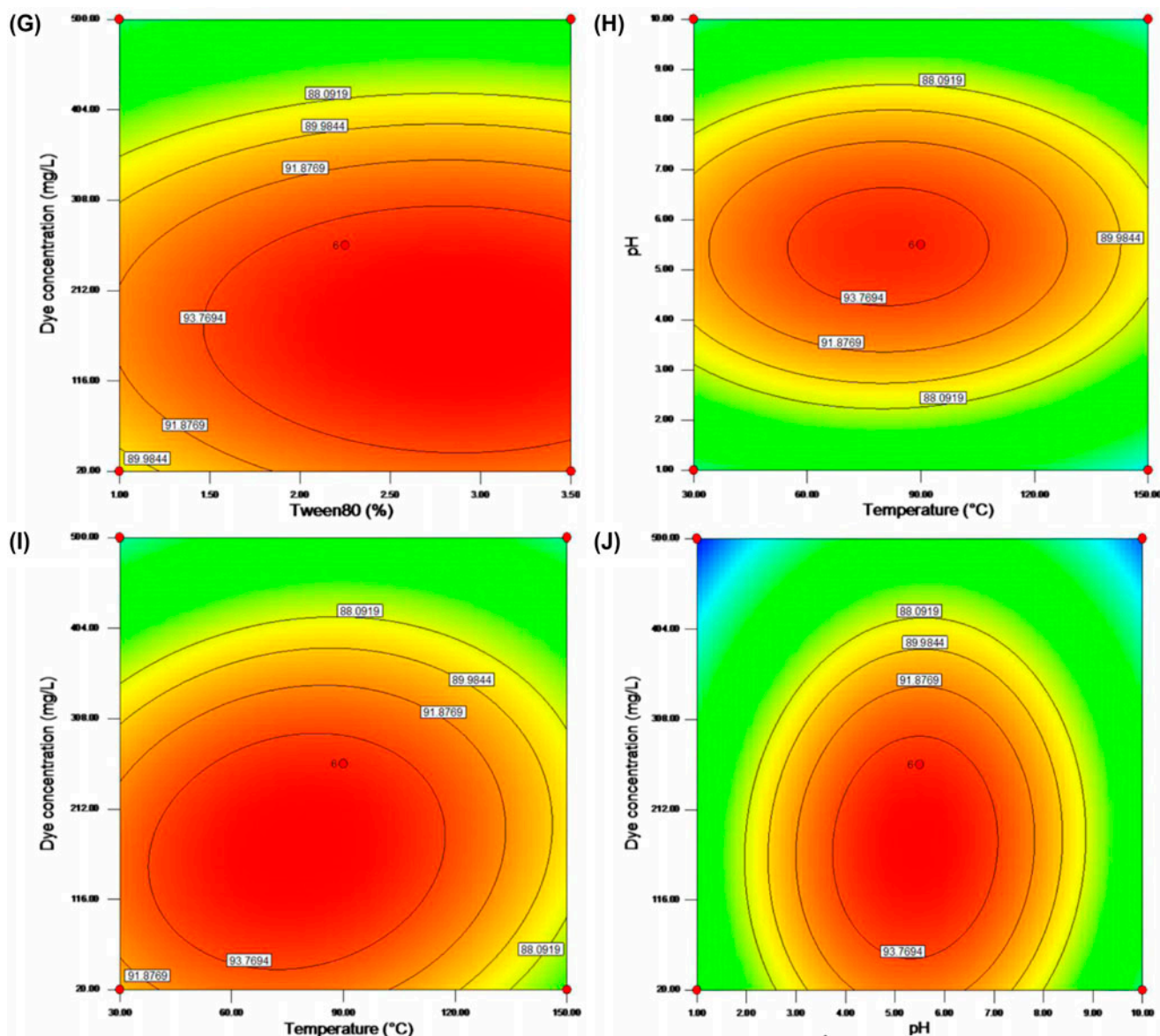


Fig. 4. (Continued)

the experimentally determined production values were in close agreement with the statistically predicted ones, confirming the model's authenticity.

### 3.4. Chemical modification

To confirm the contribution for dye biosorption made by the functional groups of the adsorbents surface, the results of the target dye Congo Red decolorization rates by adsorbents with chemical modifications were demonstrated in Fig. 5. There was no effect on Congo Red adsorptive decolorization by adsorbents without lipids (Fig. 5(A)). It was evident

that the lipids were not the dye adsorptive sites of adsorbents. Fig. 5(B) displayed that no notable changes of decolorization rate were observed compared to the control after modified by triethyl phosphate and nitromethane. It implied that phosphate groups were not involved with charges transfer. As shown in Fig. 5(C), the Congo Red decolorization efficiency decreased by 34.15% after amido methylation compared to the control. Due to the conversion from R-NH<sub>2</sub> group to R-N(CH<sub>3</sub>)<sub>2</sub> group of adsorbents surface, an decrease in accepted sites of hydron occurred and then the biosorption capacity of the adsorbents cut down obviously. However, the reduction was not

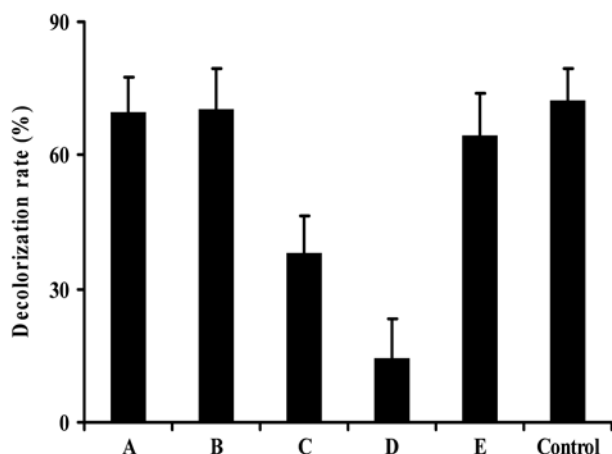


Fig. 5. Influences of the adsorbents modified by chemical methods on azo dye Congo Red decolorization rate (A) lipid removal (B) phosphate esterification (C) amido methylation (D) amido acetylation, and (E) carboxyl esterification.

extremely serious. Fig. 5(D) suggested that amido acetylation urged the adsorbents to lose their protonated sites and diminish the surface charges, thereby leading to a dramatic decrease in the electrostatic force between adsorbents and dyes. After a 7-day incubation period, the decolorization rate was merely 14.52%. Moreover, there was no influence on Congo Red decolorization rate by adsorbents modified by carboxyl esterification compared to control (Fig. 5(E)).

These results suggested that the dye adsorptive decolorization was attributed to the electrostatic attractions between negatively charged dyes and positively charged cell walls of adsorbents induced by

amido protonation [17,18]. The amido group played a major role in adsorption of azo dye Congo Red at the optimum pH value. On the contrary, desorption could be achieved by means of breaking down the electrostatic force as well.

### 3.5. Biosorption characterization

SEM photomicrographs of the adsorbents obtained from *T. pubescens* pellets before and after dye treatment were presented in Fig. 6, which confirmed that the biosorption occurred. Fig. 6(A) showed that the surface of unadsorbed *T. pubescens* adsorbent was typically wrinkled polymeric network with irregular pores. In addition, a porous internal structure was observed. After adsorption of azo dye Congo Red, adsorbent pores were not visible. This demonstrated that a dye thin layer had covered the entire external adsorbent surface and the dye had densely and homogeneously adhered to the adsorbent surface (Fig. 6(B)). These observations indicated that the dry powders obtained from *T. pubescens* pellets were very effective adsorbents due to their highly developed porosities and heterogeneous surface areas.

As demonstrated in Fig. 1(B), the FTIR spectrum of adsorbent after dye decolorization displayed several peaks, which were extremely similar to those before decolorization (Fig. 1(A)). The result indicated that the dye decolorization by the adsorbents obtained from *T. pubescens* pellets was absolutely a biosorption course, and this course did not alter any surface functional groups at all.

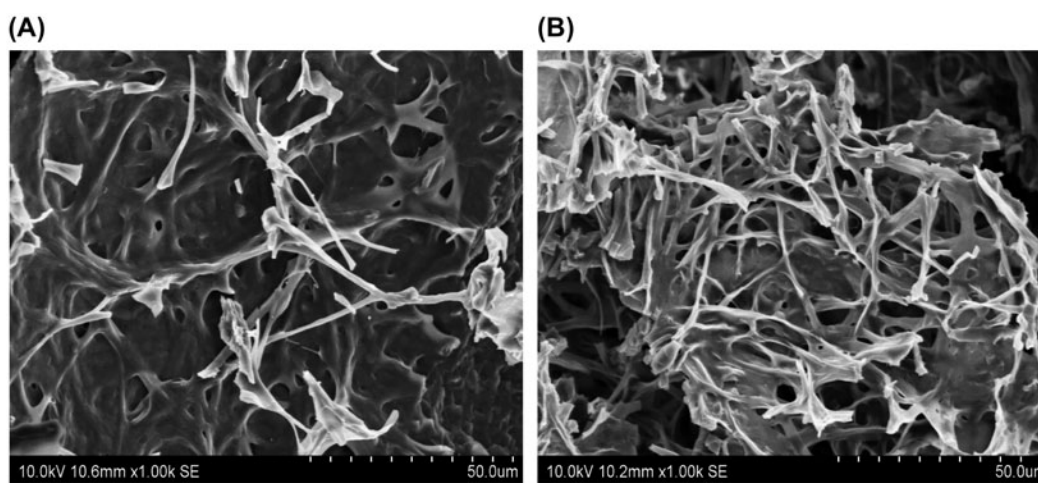


Fig. 6. SEM photomicrographs of the adsorbents obtained from *T. pubescens* pellets (A) before dye decolorization and (B) after dye decolorization.

#### 4. Conclusions

A design of the efficient color removal of dyes was conducted, with the adsorbents obtained from white rot fungus *T. pubescens* pellets prepared by moist heat sterilization. Mathematical models of BBD were developed for optimizing the effects of salinity, Tween80, temperature, pH, and dye concentration, as well as their interactions on azo dye Congo Red adsorptive decolorization. Additionally, biosorption was caused by the electrostatic forces between dye molecules and adsorbents; amido group played a major role during the biosorption process and this course did not alter any functional groups at all, as evidenced by FTIR, chemical modifications, and SEM data. These results indicated that the adsorbents obtained from *T. pubescens* pellets were suitable candidates to accelerate azo dye Congo Red decolorization.

#### Acknowledgements

This study was supported by the Fundamental Research Funds for the Central Universities (Nos. BLYJ201304, JC2013-1) and the Program for New Century Excellent Talents in University (NCET-11-0585).

#### References

- [1] A. Muhammad, K. Shahnaz, N.B. Haq, A.H.S. Syed, A. Muhammad, Optimization of medium for decolorization of Solar golden yellow R direct textile dye by *Schizophyllum commune* IBL-06, *Int. Biodeterior. Biodegrad.* 61 (2008) 189–193.
- [2] T. Deveci, A. Unyayar, M.A. Mazmanci, Production of Remazol Brilliant Blue R decolorising oxygenase from the culture filtrate of *Funalia trogii* ATCC 200800, *J. Mol. Catal. B Enzym.* 30 (2004) 25–32.
- [3] F.M. Munari, T.A. Gaio, A.J.P. Dillon, Phenol degradation and colour removal in submerged culture of *Pleurotus sajor-caju* with paper mill effluents, *Biocatal. Biotransform.* 25 (2007) 24–28.
- [4] I.M. Banat, P. Nigam, D. Singh, R. Marchant, Microbial decolorization of textile-dye-containing effluents: A review, *Bioresour. Technol.* 58 (1996) 217–227.
- [5] M.S. Revankar, S.S. Lele, Synthetic dye decolorization by white rot fungus, *Ganoderma* sp. WR-1, *Bioresour. Technol.* 98 (2007) 775–780.
- [6] H.R. Karimniaae-Hamedani, A. Sakurai, M. Sakakibara, Decolorization of synthetic dyes by a new manganese peroxidase-producing white rot fungus, *Dyes Pigm.* 72 (2007) 157–162.
- [7] Č. Novotný, N. Dias, A. Kapanen, K. Malachová, M. Vándrovcová, M. Itävaara, N. Lima, Comparative use of bacterial, algal and protozoan tests to study toxicity of azo- and anthraquinone dyes, *Chemosphere* 63 (2006) 1436–1442.
- [8] A.H. Ali, S. Kapoor, S.K. Kansal, Studies on the photocatalytic decolorization of pararosaniline chloride dye and its simulated dyebath effluent, *Desal. Wat. Treat.* 25 (2011) 268–275.
- [9] Ö. Gökkuş, M. Oğuz, Investigation of color and COD removal by Fenton reagent from aqueous solutions containing acid and reactive dyestuffs, *Desal. Wat. Treat.* 26 (2011) 160–164.
- [10] M. Chander, D.S. Arora, Evaluation of some white-rot fungi for their potential to decolorize industrial dyes, *Dyes Pigm.* 72 (2007) 192–198.
- [11] G. Ghodake, S. Jadhav, V. Dawkar, S. Govindwar, Biodegradation of diazo dye Direct brown MR by *Acinetobacter calcoaceticus* NCIM 2890, *Int. Biodeterior. Biodegrad.* 63 (2009) 433–439.
- [12] M.M. Fazli, A.R. Mesdaghinia, K. Naddafi, S. Nasser, M. Yunesian, M.M. Assadi, S. Rezaie, H. Hamzehei, Screening of factors affecting reactive blue 19 decolorization by *Ganoderma* sp. using fractional factorial experimental design, *Desal. Wat. Treat.* 22 (2010) 22–29.
- [13] V.J. Leebana, H. Santhanam, K. Geetha, A. Raj, Biodegradation of direct golden yellow, a textile dye by *Pseudomonas putida*, *Desal. Wat. Treat.* 39 (2012) 1–9.
- [14] M. Güngör, S. Yildiz, E. Demýrcý, Evaluation of efficiency analysis of waste water treatment plants and applications in Denizli, *Desal. Wat. Treat.* 26 (2011) 185–193.
- [15] R.J. Doyle, T.H. Matthews, U.N. Streips, Chemical basis for selectivity of metal ions by the *Bacillus subtilis* cell wall, *J. Bacteriol.* 143 (1980) 471–480.
- [16] S. Cengiz, F. Tanrikulu, S. Aksu, An alternative source of adsorbent for the removal of dyes from textile waters: *Posidonia oceanic* (L.), *Chem. Eng. J.* 189–190 (2012) 32–40.
- [17] S.Y. Kang, J.U. Lee, K.W. Kim, Biosorption of Cr (III) and Cr (VI) onto the cell surface of *Pseudomonas aeruginosa*, *Biochem. Eng. J.* 36 (2007) 54–58.
- [18] A.H. Sulaymon, D.W. Abbood, A.H. Ali, Competitive biosorption of phenol and lead from synthetic wastewater onto live and dead microorganisms, *Desal. Wat. Treat.* 45 (2012) 331–342.
- [19] G. McKay, J.F. Porter, G.R. Prasad, The removal of dye colors from aqueous solutions by adsorption on low-cost materials, *Water Air Soil Pollut.* 114 (1999) 423–438.
- [20] Ž. Filipović-Kovačević, L. Sipos, F. Briški, Biosorption of chromium, copper, nickel and zinc ions onto fungal pellets of *Aspergillus niger* 405 from aqueous solutions, *Food Technol. Biotechnol.* 38 (2000) 211–216.
- [21] A. Du, L. Cao, R. Zhang, R. Pan, Effects of a copper-resistant fungus on copper adsorption and chemical forms in soils, *Water Air Soil Pollut.* 201 (2009) 99–107.
- [22] A.K. Mittal, S.K. Gupta, Biosorption of cationic dyes by dead macro fungus *Fomitopsis carnae*: Batch studies, *Water Sci. Technol.* 34 (1996) 81–87.
- [23] L. Casieri, G.C. Varese, A. Anastasi, V. Prigione, K. Svobodová, V.F. Marchisio, C. Novotný, Decolorization and detoxication of reactive industrial dyes by immobilized fungi *Trametes pubescens* and *Pleurotus ostreatus*, *Folia Microbiol.* 53 (2008) 44–52.
- [24] L.F. González, V. Sarria, O.F. Sánchez, Degradation of chlorophenols by sequential biological-advanced oxidative process using *Trametes pubescens* and TiO<sub>2</sub>/UV, *Bioresour. Technol.* 101 (2010) 3493–3499.
- [25] M.S. Roriz, J.F. Osma, J.A. Teixeira, S. Rodríguez-Couto, Application of response surface methodological approach to optimize Reactive Black 5 decolouration by crude laccase from *Trametes pubescens*, *J. Hazard. Mater.* 169 (2009) 691–696.
- [26] Y.C. Dai, Polypore diversity in China with an annotated checklist of Chinese polypores, *Mycoscience* 53 (2012) 49–80.
- [27] Y.C. Dai, Z.L. Yang, B.K. Cui, C.J. Yu, L.W. Zhou, Species diversity and utilization of medicinal mushrooms and fungi in China (Review), *Int. J. Med. Mushrooms* 11 (2009) 287–302.
- [28] C.C. Oturkar, H.N. Nemade, P.M. Mulik, M.S. Patole, R.R. Hawaldar, K.R. Gawai, Mechanistic investigation of decolorization and degradation of Reactive Red 120 by *Bacillus lentus* BI377, *Bioresour. Technol.* 102 (2011) 758–764.
- [29] H. Pathak, S. Patel, M. Rathod, K. Chauhan, In vitro studies on degradation of synthetic dye mixture by *Comamonas* sp. VS-MH2 and evaluation of its efficacy using simulated microcosm, *Bioresour. Technol.* 102 (2011) 10391–10400.
- [30] G.H. Sonawane, V.S. Shrivastava, Removal of hazardous dye from synthetic textile dyeing and printing effluents by *Archis hypogaea* L. shell: A low cost agro waste material, *Desal. Wat. Treat.* 29 (2011) 29–38.

- [31] D.P. Tamboli, A.N. Kagalkar, M.U. Jadhav, J.P. Jadhav, S.P. Govindwar, Production of polyhydroxyhexadecanoic acid by using waste biomass of *Sphingobacterium* sp. ATM generated after degradation of textile dye Direct Red 5B, *Bioresour. Technol.* 101 (2010) 2421–2427.
- [32] O.M. Gomaa, J.E. Linz, C.A. Reddy, Decolorization of Victoria blue by the white rot fungus, *Phanerochaete chrysosporium*, *World J. Microbiol. Biotechnol.* 24 (2008) 2349–2356.
- [33] Z. Aksu, A. Çalik, A.Y. Dursun, Z. Demircan, Biosorption of iron (III)-cyanide complex anions to *Rhizopus arrhizus*: Application of adsorption isotherms, *Process Biochem.* 34 (1999) 483–491.
- [34] Z. Aksu, S. Tezer, Equilibrium and kinetic modelling of biosorption of Remazol Black B by *Rhizopus arrhizus* in a batch system: Effect of temperature, *Process Biochem.* 36 (2000) 431–439.
- [35] A.R. Khataee, B. Habibi, Photochemical oxidative decolorization of CI basic red 46 by UV/H<sub>2</sub>O<sub>2</sub> process: Optimization using response surface methodology and kinetic modeling, *Desal. Wat. Treat.* 16 (2010) 243–253.
- [36] S. Chowdhury, P. Das, Scale-up of a dye adsorption process using chemically modified rice husk: Optimization using response surface methodology, *Desal. Wat. Treat.* 37 (2012) 331–336.
- [37] I. Fernández-Silva, P. Sanmartín, B. Silva, A. Moldes, B. Prieto, Quantification of phototrophic biomass on rocks: Optimization of chlorophyll-*a* extraction by response surface methodology, *J. Ind. Microbiol. Biotechnol.* 38 (2011) 179–188.
- [38] M. Kousha, E. Daneshvar, H. Dopeikar, D. Taghavi, A. Bhatnagar, Box–Behnken design optimization of Acid Black 1 dye biosorption by different brown macroalgae, *Chem. Eng. J.* 179 (2012) 158–168.
- [39] R.O. Cristóvão, P.F.F. Amaral, A.P.M. Tavares, M.A.Z. Coelho, M.C. Cammarota, J.M. Loureiro, R.A.R. Boaventura, E.A. Macedo, F.L.P. Pessoa, Optimization of laccase catalyzed degradation of reactive textile dyes in supercritical carbon dioxide medium by response surface methodology, *Reac. Kinet. Mech. Cat.* 99 (2010) 311–323.
- [40] J.D. Cui, Optimization of medium for phenylalanine ammonia lyase production in *E. coli* using response surface methodology, *Korean J. Chem. Eng.* 27 (2010) 174–178.
- [41] J. Zhong, C. Liu, W. Liu, X. Cai, Z. Tu, J. Wan, Effect of dynamic high-pressure microfluidization at different temperatures on the antigenic response of bovine  $\beta$ -lactoglobulin, *Eur. Food Res. Technol.* 233 (2011) 95–102.